

TDP-43 の凝集に関わる配列

研究分担者：久永 眞市¹

研究協力者：下中 翔太郎^{1,2}、野中 隆²、長谷川 成人²

1. 首都大学東京 理工学研究科生命科学専攻 神経分子機能研究室
2. 公益財団法人東京都医学総合研究所 認知症・高次脳機能分野 病態細胞生物研究室

前頭側頭葉変性症(FTLD)、筋萎縮性側索硬化症(ALS)などの病変部位に見られるユビキチン陽性封入体(UbIs)の主成分として、核蛋白である TDP-43 が同定されたことから、これらの疾患と、TDP-43 との関連性が示されている。全長 TDP-43 の C 末端側断片を SH-SY5Y 細胞に発現させると、細胞内に凝集体が形成されるが、その凝集体形成のメカニズムについては未だに明らかになっていない。本研究では、TDP-43 の凝集に関わる配列の同定を試みた。GFP タグ付 TDP-C 末端断片(162-414)の部分欠損変異体を SH-SY5Y 細胞に一過性に発現させ、蛍光顕微鏡観察とイムノブロット解析により、凝集体形成に影響する配列を探索した結果、glycine-rich domain の 274-293、294-313 を欠損させると凝集体形成が著しく阻害されることを見いだした。次に、それらの配列のペプチドを合成し、37°Cで振盪後、thioflavin S 蛍光測定、電子顕微鏡観察、培養細胞モデルへの導入により、その線維形成能、シード能を検討した。その結果、274-313 のペプチドは、Thioflavin S 陽性の線維構造を形成し、また SY5Y 細胞内に導入すると、全長 TDP-43 を凝集させるシード能を有することが明らかになった。以上のことから、274-313 の配列そのものが強い凝集能を有しており、TDP-43 の凝集、及びその伝播において中心的な役割を担っていることが示唆された。

A.研究目的

前頭側頭葉変性症(FTLD)、筋萎縮性側索硬化症(ALS)などの神経変性疾患において、病理構造物であるユビキチン陽性封入体(UbIs)がその病変部位に認められる。本研究では UbIs の主要蛋白である TDP-43 に着目し、UbIs の形成に必要な配列を同定することで、病理構造物形成のメカニズム解明への足がかりとすることを目的とした。

B.研究方法

TDP-43 の C 末端側の断片(162-414)について 214 残基から 414 残基まで、20 残基ずつを順に欠損させた変異体を、GFP との融合蛋白として 9 種作製した。これらの変異体と、欠損なしの断片をヒト神経芽細胞 SH-SY5Y にトランスフェクションし、CO₂ インキュベータ内で 37°Cにてインキュベートした。

2 日後、蛍光顕微鏡を用いて、欠損なしの断片

と各種の変異体を一過性に発現させた細胞について、それぞれ 488nm の波長で GFP の蛍光を観察した。得られた画像に対して、明るい凝集体の蛍光だけを検出するように閾値を設定し輝度抽出を行い、得られた輝度を積算して凝集体形成を定量化した。

次に、界面活性剤である Sarkosyl(Sar)を 1%含むバッファーで細胞を回収、超音波処理をした後超遠心の操作により細胞ライセートを Sar 可溶性(sup)、Sar 不溶性(ppt)とに分画した。次に、それぞれの画分に対して、抗 GFP 抗体、抗リン酸化 TDP-43 抗体(pS409/410: 疾患中に見られる異常リン酸化部位に対する抗体)を用いてイムノブロットを行った。

以上の実験の結果、同定された TDP-43 の 274-313、294-313 の配列を元に、Sigma Aldrich 社に依頼して 274-313 と、そのコントロールとして 234-373、314-353、及びランダムペプチド(40 残基)

の計4種のペプチドを合成した。

これらのペプチドの溶液をシェーカー上で37°Cにて震盪し、調製直後の0日、1、4、8日後に少量採取したものを5 μ MのThioflavin S溶液に添加し、 λ_{ex} = 436nm、 λ_{em} = 535nmの蛍光を測定した。また、8日以上振盪したペプチド溶液中の線維を、リンタングステン酸でネガティブ染色の処理をした後、透過型電子顕微鏡により観察した。

また、SY5Y細胞に対して、全長TDP-43をコードしたプラスミドとペプチド線維をトランスフェクション試薬であるMultiFectamを用いて同時に導入し、2日後に細胞ライセートのSarkosyl不溶性画分を調製、抗リン酸化TDP-43抗体でイムノブロットを行った。

(倫理面への配慮)

本研究は、それぞれの所属施設において、遺伝子組換え生物等・病原体等実験計画書を提出し、承認を受けて行った。

C.研究結果

GFP-TDP43C断片のglycine-rich domain上の274-293、294-313、Q/N-rich domain上の354-373を欠損した断片を発現した場合にTDP-43C末端断片の凝集能が著しく低下することが判明した。さらに、これらのペプチドと周辺の配列を合成し、37°Cでインキュベートしたところ、274-313と314-353のペプチドがチオフラビンS陽性、かつ電子顕微鏡で確認できる明確な線維構造を形成することが判明した。

次いで、全長TDP-43をコードしたプラスミドをトランスフェクションすると同時に、ペプチド線維をSY5Y細胞内に導入した結果、274-313、314-353の線維が凝集核として働き、細胞内に過剰発現させた全長TDP-43を凝集させ、患者脳と類似のリン酸化TDP-43陽性TDP43の蓄積とその断片化が観察された。さらにその断片のバンドパターンには両者で違いが認められた。

D.考察

TDP-43のC末端の274-293、294-313の配列の欠損によって、GFP-TDP43C断片(162-414)の凝集体形成能は劇的に減少したことと、この配列に基づいて合成した274-313の合成ペプチドが、それ自体でアミロイド線維を形成することが判明した。さらに、培養細胞に導入したところ、細胞内に発現する全長TDP-43を凝集させるシード能を有することも明らかとなった。従って、この配列そのものが高い凝集能を持ち、TDP-43の凝集体形成過程において中心的な役割を果たしていると考えられた。

E.結論

TDP-43の274-313の配列は、配列そのものが強い凝集能を有しており、TDP-43の凝集、及びその伝播において中心的な役割を担っていることが示唆された。

「TDP-43の凝集阻害」というFTLD、ALSの分子レベルでの治療戦略にはTDP-43の凝集メカニズムの理解が必要であるが、凝集に必要とされる配列を同定した本研究は、凝集メカニズムの解明に大きく貢献できると考えられる。

F.健康危険情報

特になし

G.研究発表

(発表誌名巻号・頁・発行年等も記入)

1.論文発表

1. Kimura et al, Pin1 Stimulates Dephosphorylation of Tau at Cdk5-Dependent Alzheimer Phosphorylation Sites. *J. Biol. Chem.*288, 7968-7977, 2013.
2. Fuchigami et al, Dab1-mediated colocalization of multi-adaptor protein CIN85 with Reelin-receptors, ApoER2 and VLDLR, in neurons. *Gene to Cells* 18. 410-424, 2013.
3. Nagano et al. Cyclin I is involved in the regulation of cell cycle progression. *Cell Cycle* 12, 2617-2624,

2013.

4. Saito et al. Structural basis for the different stability and activity between the Cdk5 complexes with p35 and p39 activators. J. Biol. Chem.288, 32433-32439, 2013.
5. Asada et al. Cyclin-dependent kinase 5 phosphorylates and induces the degradation of ataxin-2. Neurosci Lett in press

2.学会発表

- ・第17回武田科学振興財団生命科学シンポジウム(ポスター発表)
- ・第85回日本生化学会大会(口頭・ポスター発表)
- ・第3回 TOBIRA 研究交流フォーラム(ポスター発表)

H.知的財産権の出願・登録状況(予定を含む)

1.特許取得

なし

2.実用新案登録

なし

3.その他

特になし

霊長類 ALS タンパク伝播モデル作製の試み

研究分担者： 横田隆徳¹⁾
共同研究者： 大久保卓哉¹⁾，田尻美緒¹⁾，寺岡静香¹⁾，宮田悠¹⁾，
阿部圭輔¹⁾，関口輝彦¹⁾，内原俊記²⁾，水澤英洋¹⁾，
野中隆³⁾

- 1) 東京医科歯科大学大学院 脳神経病態学（神経内科）
- 2) 東京都医学総合研究所 脳病理形態研究室
- 3) 東京都医学総合研究所 認知症プロジェクト

研究要旨

我々が構築した世界初の霊長類 ALS モデルにおいて、逆行性輸送による蛋白伝播の可能性を証明すべく、ALS 患者脳から蛋白不溶性画分を抽出してサル脊髄に直接注入することにより、蛋白伝播霊長類モデルを新たに構築することを試みた。ALS 患者剖検脳前頭葉皮質約 0.5g からサルコシル不溶性蛋白画分を抽出し、タグ無し全長 TDP-43 を発現させた SH-SY5Y 細胞に、このサルコシル不溶性画分をトランスフェクションし、細胞から抽出した蛋白画分をイムノブロットすることで、シード効果を確認した。続いてカニクイザル 2 頭に対して麻酔下に椎弓切除術を行い、第 6 頸髄の利き手側の前角細胞付近に、ALS 患者脳および非 ALS 患者脳から抽出したサルコシル不溶性蛋白画分を注入した。麻痺症状は出現せず、注入 32 週後に解剖し、神経病理学的検査を行ったが、TDP-43 の異常局在やリン酸化の所見は認められなかった。

A. 研究目的

我々は孤発性 ALS における野生型 TDP-43 の病態を解明すべく、カニクイザルの頸髄前角に pAAV-IRES-hrGFP ベクターを用いて野生型 TDP-43 と hrGFP を過剰発現させ、脊髄および脳を含めた TDP-43 の拡がりを確認した。しかし、この実験系ではウイルス自体の拡がり完全に否定できないため、孤発性 ALS 患者脳から抽出したサルコシル不溶性蛋白画分をサル脊髄に注入し、その画分に含まれる TDP-43 の拡がりを解析することを着想した。

B. 研究方法

まず ALS 患者剖検脳 3 例(ALS1-3)の前頭葉皮質約 0.5g からサルコシル不溶性蛋白画分を抽出し、ウ

ェスタンブロット法にて TDP-43 の存在を確認した（図 1）。次に、SH-SY5Y 細胞にタグ無し全長 TDP-43 をトランスフェクションし、24 時間後にこのサルコシル不溶性画分をトランスフェクションした。2 日間培養して細胞を回収し、トリス可溶性、TritonX100 可溶性、サルコシル可溶性、不溶性画分に分けてイムノブロットし、シード効果を確認した。3 例のうち ALS2 及び ALS3 の 2 症例で TDP-43 のシード効果が強いことが判明したが、陽性対照 ALS 例と比較すると蛋白量がやや少なかったため、2 例分のサルコシル不溶性画分を合わせてカニクイザル脊髄に注入することとした（図 2）。

続いてカニクイザル 2 頭に対して麻酔下に椎弓切除術を行い、第 6 頸髄の利き手側の前角細胞付近に、

1 頭は孤発性 ALS 患者脳から抽出し、培養細胞系でシード効果が確認できたサルコシル不溶性蛋白画分 (5 μ l), もう 1 頭は対照として、非 ALS 患者脳から抽出したサルコシル不溶性蛋白画分(5 μ l)を注入した。アップルテストなどの行動解析に加え、前肢筋の針筋電図や正中神経の末梢神経伝導検査を行い、注入 32 週後に解剖し、神経病理学的検査を行った。

(倫理面への配慮) 医薬基盤研究所霊長類医科学研究センターでは、長年に渡る霊長類を用いた動物モデル研究により培った技術に基づいて実験を行い、特に外科手術や安楽死ではサル之苦痛を最小限にする配慮を行った (承認番号: DS24-20)。

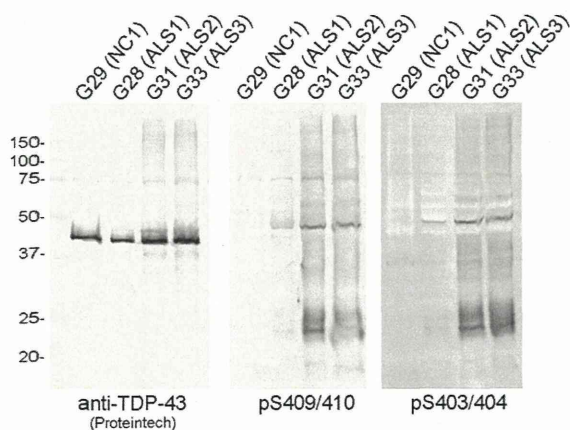


図 1. ヒト脳サルコシル不溶性画分のイムノブロット (ALS3 例; ALS1-3, 疾患対照 1 例; NC1).

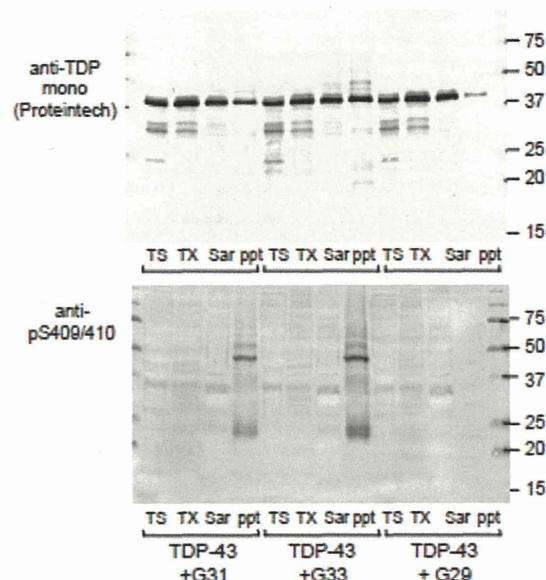


図 2. ヒト脳サルコシル不溶性画分の TDP-43 発現 SH-SY5Y 細胞におけるシード実験. ALS2(G31), ALS3(G33)でシード効果を確認した (0113; 陽性対照 ALS 脳).

C. 研究結果

32 週の経過観察を行ったが、明らかな麻痺は出現せず、アップルテストや行動解でも異常は認められなかった。また、電気生理学的には正中神経刺激による複合筋活動電位の低下は認められず、病理所見でも TDP-43 の異常局在およびリン酸化 TDP-43 の染色性は認められなかった。

D. 考察

サル未発症およびタンパクの拡がり認められなかった原因としては、注入蛋白量の問題あるいはヒトとサルの種の壁の問題の可能性があり、今後検討の余地がある。

E. 結論

本サルモデル研究では明らかな phenotype が出るところまで達成しておらず、注入蛋白量や画分のさらなる検討が必要と考えられた。

F.健康危険情報

なし

G.研究発表

1.論文発表

1. Machida A, Ohkubo T, Yokota T. Circulating microRNAs in the cerebrospinal fluid of patients with brain diseases. In: Kosaka N eds., Circulating miRNAs, Methods in Molecular Biology, Humana Press, Springer Science+Business Media, New York, 2013; 1024: 203-209. (doi: 10.1007/978-1-62703-453-1_16.)
2. Sekiguchi T, Kanouchi T, Shibuya K, Noto YI, Yagi Y, Inaba A, Abe K, Misawa S, Orimo S, Kobayashi T, Kamata T, Nakagawa M, Kuwabara S, Mizusawa H, Yokota T. Spreading of amyotrophic lateral sclerosis lesions--multifocal hits and local propagation? J Neurol Neurosurg Psychiatry 2013 ; (doi: 10.1136/jnnp-2013-305617.)

2.学会発表

1. 大久保卓哉, 田尻美緒, 関口輝彦, 寺岡静香, 木村展之, 内原俊記, 水澤英洋, 横田隆徳. 霊長類 ALS モデルにおける TDP-43 の拡がり. 第 54 回日本神経学会学術大会. 東京. 2013.5.31.
2. 阿部圭輔, 大久保卓哉, 水澤英洋, 横田隆徳. 筋萎縮性側索硬化症患者皮膚における TDP-43 の発現について. 第 54 回日本神経学会学術大会. 東京. 2013. 5. 30.
3. 町田明, 大久保卓哉, 松尾秀徳, 水澤英洋, 横田隆徳. 筋萎縮性側索硬化症における髄液 microRNA プロファイリング解析. 第 5 回 RNAi 研究会. 広島. 2013. 8. 29.

4. 大久保卓哉, 横田隆徳. 筋萎縮性側索硬化症における新規髄液バイオマーカーの検索. 第 7 回川棚神経科学の会. 長崎. 2013.12.6.

H.知的所有権の取得状況 (予定を含む)

- 1.特許取得
なし
- 2.実用新案登録
なし
- 3.その他
なし

表題：TDP-43 量は自己 mRNA の polyA 選択、スプライシング、核貯留の協働
により制御される

須貝章弘¹⁾、小山哲秀²⁾、加藤泰介¹⁾、志賀篤³⁾、今野卓哉¹⁾

小山美咲¹⁾、石原智彦¹⁾、西澤正豊¹⁾、小野寺理⁴⁾

1) 新潟大学脳研究所神経内科

2) 新潟大学研究推進機構超域学術院

3) 新潟大学脳研究所病理学分野

4) 新潟大学脳研究所分子神経疾患資源解析学分野

研究要旨

筋萎縮性側索硬化症（ALS）関連蛋白である TDP-43 の量の異常は神経細胞死をきたす。一方、正常細胞において、TDP-43 は一定量に制御されている。我々はこれまでに、TDP-43 の増加時には、TDP-43 が自己 pre-mRNA 3' UTR へ結合し、遠位 polyA 付加部位の使用を誘導し、さらに exon6 内で複数のスプライシングを惹起することにより、ナンセンス依存性 mRNA 分解機構（NMD）を介した自己 mRNA の分解を引き起こし、自らの発現量を低下させることを明らかにしている。今回我々は、ALS 罹患組織で認められる核内 TDP-43 の減少状態における TDP-43 mRNA の動態を明らかにした。核内 TDP-43 が減少すると、核内に保持されている遠位 polyA 付加部位を使用した TDP-43 mRNA が細胞質に移行する。これに加え、新しく転写される mRNA は、近位 polyA 付加部位を使用し、exon6 内のスプライシングが抑制され、細胞質に移行する。この 2 段階の細胞質内 TDP-43 mRNA を増加させる量的制御機構が TDP-43 減少時に働いている。

A. 研究目的

筋萎縮性側索硬化症（ALS）関連蛋白である TDP-43 は、正常細胞において一定量に制御される。一方、TDP-43 の過剰発現系では神経細胞死がもたらされる。このことは、TDP-43 の量の異常に神経細胞が脆弱である可能性を示唆している。我々はこれまでに、TDP-43 の増加時には、TDP-43 が自己 pre-mRNA 3' UTR へ結合し、遠位 polyA 付加部位の使用を誘導し、さらに exon6 内で複数のスプライシングを惹起することにより、ナンセンス依存性 mRNA 分解機構（NMD）を介した自己 mRNA の分解を引き起こし、発現量を低下させることを明らかにしている。しかし、ALS 病理では TDP-43 は核内で減少している状態にある。この自己 mRNA を介した協調的な自己制御機構が ALS 病理にどの

ように関与しているのかは明らかではない。今回、我々は、TDP-43 減少時における TDP-43 mRNA の動態を明らかにすることを目的とした。

B. 研究方法

TDP-43 exon6 を含むミニジーンを作成し、HEK293T 細胞にトランスフェクションした。siRNA により内在性 TDP-43 をノックダウンし、これに伴うミニジーン由来の mRNA を、ノザンブロットイングおよび定量リアルタイム PCR により解析した。

C. 研究結果

内在性 TDP-43 と同様に、ミニジーン由来の転写産物においても、遠位 polyA 付加部位を使用した

mRNA が核内に存在する割合が多かった。TDP-43 減少時には、この核内の mRNA が細胞質へ移行した。さらにこのとき、近位 polyA 付加部位を使用した mRNA の割合が増加することを示した。これに伴い exon6 内で複数のスプライシングを受けて NMD にまわる mRNA の減少を認めた。これらにより、TDP-43 発現亢進に寄与する細胞質内 mRNA の増加を認めた。

D. 考察

我々は、TDP-43 減少時における TDP-43 発現亢進機構を明らかにした。この TDP-43 の制御機構が ALS 罹患組織においても働いているならば、ALS で早期から認めるとされる核内 TDP-43 の減少・消失は、細胞質内 TDP-43 mRNA 増加をもたらすことにより、TDP-43 の発現亢進をきたし、細胞質内での封入体形成を加速させている可能性がある。逆に、この自己制御機構が ALS 罹患組織において機能していなければ、核内 TDP-43 の減少状態が継続し、細胞機能の低下をもたらしている可能性がある。今後、ALS 罹患組織における TDP-43 mRNA の動態を解明することにより、ALS 病態の理解が深まるものと考えられる。

E. 結論

核内 TDP-43 が減少すると、核内に保持されている遠位 polyA 付加部位を使用した TDP-43 mRNA が細胞質に移行する。これに加え、新しく転写される mRNA は、近位 polyA 付加部位を使用し、exon6 内のスプライシングが抑制される。この2段階の細胞質内 TDP-43 mRNA を増加させる量的制御機構が TDP-43 減少時に働いている。

F. 健康危険情報

なし

G. 研究発表

(発表誌名巻号・頁・発行年等も記入)

1. 論文発表

2. 学会発表

1) 須貝 章弘、小山 哲秀、今野 卓哉、加藤 泰介、西澤 正豊、小野寺 理：TDP-43 量は TDP-43 に惹起される自己 mRNA のスプライシングで制御される：第 54 回日本神経学会学術大会（2013 年 5 月、東京）

2) 小山 哲秀、須貝 章弘、今野 卓哉、加藤 泰介、石原 智彦、西澤 正豊、小野寺 理：TDP-43 は mRNA の自己調節機構を介して自身の蛋白量を制御する：包括脳ネットワーク 2013 年度夏のワークショップ（2013 年 8 月、名古屋）

3) Akihiro Sugai, Akihide Koyama, Taisuke Kato, Takuya Konno, Tomohiko Ishihara, Masatoyo Nishizawa, Osamu Onodera: Alternative splicing or polyadenylation, which is the major mechanism for auto-regulation of TDP-43? : RNA Metabolism in Neurological Disease: 8th Brain Research Conference (November 2013, San Diego)

4) Akihiro Sugai, Akihide Koyama, Taisuke Kato, Takuya Konno, Tomohiko Ishihara, Masatoyo Nishizawa, Osamu Onodera: Alternative splicing or polyadenylation, which is the major mechanism for auto-regulation of TDP-43? : Society for Neuroscience 43rd Annual Meeting (November 2013, San Diego)

5) Akihide Koyama, Akihiro Sugai, Taisuke Kato, Takuya Konno, Tomohiko Ishihara, Masatoyo Nishizawa, Osamu Onodera: TDP-43 is autoregulated by multiple excisions of introns in exon6 and reservation of mRNA in nucleus by TDP-43 : 24th International Symposium on ALS/MND (December 2013, Milan)

H. 知的財産権の出願・登録状況（予定を含む）

1. 特許取得

なし

2.実用新案登録

なし

3.その他

なし

【研究成果の刊行に関する一覧表】

原著・症例報告

著者名	論文タイトル名	雑誌名	巻・号	ページ	出版年
Hosokawa M, Arai T, Yamashita M, Tsuji H, Nonaka T, Masuda-Suzukake M, Tamaoka A, Hasegawa M, Akiyama H.	Differential diagnosis of amyotrophic lateral sclerosis from Guillain-Barré syndrome by quantitative determination of TDP-43 in cerebrospinal fluid.	Int J Neurosci.			in press
Hasegawa M, Watanabe S, Kondo H, Akiyama H, Mann DM, Saito Y, Murayama S.	3R and 4R tau isoforms in paired helical filaments in Alzheimer's disease.	Acta Neuropathol.	127	303-5	2014
Mann DM, Rollinson S, Robinson A, Bennion Callister J, Thompson JC, Snowden JS, Gendron T, Petrucelli L, Masuda-Suzukake M, Hasegawa M, Davidson Y, Pickering-Brown S.	Dipeptide repeat proteins are present in the p62 positive inclusions in patients with frontotemporal lobar degeneration and motor neurone disease associated with expansions in <i>C9ORF72</i> .	Acta Neuropathol Commun.	1	68	2013
Dan A, Takahashi M, Masuda-Suzukake M, Kametani F, Nonaka T, Kondo H, Akiyama H, Arai T, Mann DM, Saito Y, Hatsuta H, Murayama S, Hasegawa M.	Extensive deamidation at asparagine residue 279 accounts for weak immunoreactivity of tau with RD4 antibody in Alzheimer's disease brain.	Acta Neuropathol Commun.	1	54	2013
Liu R, Yang G, Nonaka T, Arai T, Jia W, Cynader MS.	Reducing TDP-43 aggregation does not prevent its cytotoxicity.	Acta Neuropathol Commun.	1	49	2013
Nonaka T, Masuda-Suzukake M, Arai T, Hasegawa Y, Akatsu H, Obi T, Yoshida M, Murayama S, Mann DM, Akiyama H, Hasegawa M.	Prion-like properties of pathological TDP-43 aggregates from diseased brains.	Cell Rep.	4	124-34	2013
Moujalled D, James JL, Parker SJ, Lidgerwood GE, Duncan C, Meyerowitz J, Nonaka T, Hasegawa M, Kanninen KM, Grubman A, Liddell JR, Crouch PJ, White AR.	Kinase Inhibitor Screening Identifies Cyclin-Dependent Kinases and Glycogen Synthase Kinase 3 as Potential Modulators of TDP-43 Cytosolic Accumulation during Cell Stress.	PLoS One.	8	e67433	2013
Kobayashi Z, Akaza M, Ishihara S, Tomimitsu H, Inadome Y, Arai T, Akiyama H, Shintani S.	Thalamic hypoperfusion in early stage of progressive supranuclear palsy (Richardson's syndrome): Report of an autopsy-confirmed case.	J Neurol Sci.	335	224-7	2013
Kobayashi Z, Kawakami I, Arai T, Yokota O, Tsuchiya K, Kondo H, Shimomura Y, Haga C, Aoki N, Hasegawa M, Hosokawa M, Oshima K, Niizato K, Ishizu H, Terada S, Onaya M, Ikeda M, Oyanagi K, Nakano I, Murayama S, Akiyama H, Mizusawa H.	Pathological features of FTL-D-FUS in a Japanese population: Analyses of nine cases.	J Neurol Sci.	335	89-95	2013
Kuwahara H, Tsuchiya K, Kobayashi Z, Inaba A, Akiyama H, Mizusawa H.	Cryptococcal meningitis accompanying lymphocytic inflammation predominantly in cerebral deep white matter: A possible manifestation of immune reconstitution inflammatory syndrome.	Neuropathology.	34	45-8	2013

著者名	論文タイトル名	雑誌名	巻・号	ページ	出版年
Higashi S, Kabuta T, Nagai Y, Tsuchiya Y, Akiyama H, Wada K.	TDP-43 associates with stalled ribosomes and contributes to cell survival during cellular stress.	J Neurochem.	126	288-300	2013
Takeuchi R, Toyoshima Y, Tada M, Shiga A, Tanaka H, Shimohata M, Kimura K, Morita T, Kakita A, Nishizawa M, Takahashi H.	Transportin 1 accumulates in FUS inclusions in adult-onset ALS without <i>FUS</i> mutation.	Neuropathol Appl Neurobiol.	39	580-4	2013
Shimizu H, Toyoshima Y, Shiga A, Yokoseki A, Arakawa K, Sekine Y, Shimohata T, Ikeuchi T, Nishizawa M, Kakita A, Onodera O, Takahashi H.	Sporadic ALS with compound heterozygous mutation in the <i>SQSTM1</i> gene.	Acta Neuropathol.	126	453-9	2013
Kimura T, Jiang H, Konno T, Seto M, Iwanaga K, Tsujihata M, Satoh A, Onodera O, Kakita A, Takahashi H.	Bunina bodies in motor and non-motor neurons revisited: a pathological study of an ALS patient after long-term survival on a respirator	Neuropathology.			in press
Tsujii H, Iguchi Y, Furuya A, Kataoka A, Hatsuta H, Atsuta N, Tanaka F, Hashizume Y, Akatsu H, Murayama S, Sobue G and Yamanaka K.	Spliceosome integrity is defective in the motor neuron diseases ALS and SMA.	EMBO Mol Med.	5	221-34	2013
Kakuda N, Akazawa K, Hatsuta H, Murayama S, Ihara Y. The Japanese Alzheimer's Disease Neuroimaging Initiative.	Suspected limited efficacy of γ -secretase modulators.	Neurobiol Aging.	34	1101-4	2013
Riku Y, Ikeuchi T, Yoshino H, Mimuro M, Mano K, Goto Y, Hattori N, Sobue G, Yoshida M.	Extensive aggregation of α -synuclein and tau in juvenile-onset neuroaxonal dystrophy: an autopsied individual with a novel mutation in the PLA2G6 gene-splicing site.	Acta Neuropathol Commun.	1	12	2013
Iwasaki Y, Mori K, Ito M, Tatsumi S, Mimuro M, Yoshida M.	Senile onset frontotemporal lobar degeneration with TAR-DNA binding protein 43 proteinopathy primarily presenting with wasteful habits.	Psychogeriatrics.	13	260-4	2013
Tatsumi S, Mimuro M, Iwasaki Y, Takahashi R, Kakita A, Takahashi H, Yoshida M.	Argyrophilic grains are reliable disease-specific features of corticobasal degeneration.	J Neuropathol Exp Neurol.	73	30-8	2014
Kon T, Mori F, Tanji K, Miki Y, Toyoshima Y, Yoshida M, Sasaki H, Kakita A, Takahashi H, Wakabayashi K.	ALS-associated protein FIG4 is localized in Pick and Lewy bodies, and also neuronal nuclear inclusions, in polyglutamine and intranuclear inclusion body diseases.	Neuropathology.	34	19-26	2014
Fuchigami T, Sato Y, Tomita Y, Takano T, Miyauchi SY, Tsuchiya Y, Saito T, Kubo K, Nakajima K, Fukuda M, Hattori M, Hisanaga S.	Dab1-mediated colocalization of multi-adaptor protein CIN85 with Reelin receptors, ApoER2 and VLDLR, in neurons.	Genes Cells.	18	410-24	2013
Nagano T, Hashimoto T, Nakashima A, Hisanaga S, Kikkawa U, Kamada S.	Cyclin I is involved in the regulation of cell cycle progression.	Cell Cycle.	12	2617-24	2013
Saito T, Yano M, Kawai Y, Asada A, Wada M, Doi H, Hisanaga S.	Structural basis for the different stability and activity between the Cdk5	J Biol Chem.	288	32433-9	2013

著者名	論文タイトル名	雑誌名	巻・号	ページ	出版年
	complexes with p35 and p39 activators.				
Asada A, Yamazaki R, Kino Y, Saito T, Kimura T, Miyake M, Hasegawa M, Nukina N, Hisanaga SI.	Cyclin-dependent kinase 5 phosphorylates and induces the degradation of ataxin-2.	Neurosci Lett.	563	112-7	2014
Sekiguchi T, Kanouchi T, Shibuya K, Noto Y, Yagi Y, Inaba A, Abe K, Misawa S, Orimo S, Kobayashi T, Kamata T, Nakagawa M, Kuwabara S, Mizusawa H, Yokota T.	Spreading of amyotrophic lateral sclerosis lesions--multifocal hits and local propagation?	J Neurol Neurosurg Psychiatry.	85	85-91	2014
Ishihara T, Ariizumi Y, Shiga A, Kato T, Tan CF, Sato T, Miki Y, Yokoo M, Fujino T, Koyama A, Yokoseki A, Nishizawa M, Kakita A, Takahashi H, Onodera O.	Decreased number of Gemini of coiled bodies and U12 snRNA level in amyotrophic lateral sclerosis.	Hum Mol Genet.	22	4136-47	2013

総説

著者名	論文タイトル名	雑誌名	巻・号	ページ	出版年
Onodera O, Ishihara T, Shiga A, Ariizumi Y, Yokoseki A, Nishizawa M.	Minorsplicing pathway is not minor any more: Implications for the pathogenesis of motor neuron diseases.	Neuropathology.	34	99-107	2014
野中隆, 長谷川成人	患者脳に蓄積したTDP-43のプリオン様性質	Dementia Japan	28	28-34	2014
野中隆, 長谷川成人	脳内に蓄積した TDP-43 凝集体のプリオン様性質	細胞工学	32	1076-8	2013
野中隆, 長谷川成人	細胞内異常タンパク質凝集体の細胞間伝播: 神経変性疾患の病態進行に関する新たなメカニズム	基礎老化研究	37	7-11	2013
細川雅人, 新井哲明	疾患とその病態 前頭側頭葉変性症の病理と関連遺伝子	Clinical Neuroscience	31	1435-7	2013
新井哲明	認知症性疾患の病理・分子対応	Cognition and Dementia	12	48-55	2013
吉田眞理	タウオパチーの神経病理学	Brain Nerve	65	1445-58	2013
斎藤太郎, 久永眞市	神経細胞におけるCDK5の機能とその異常活性化による神経変性疾患	実験医学	31	265-70	2013
小野寺理	TDP-43時代のALS病態研究の最前線	臨床神経学	53	1077-9	2013

単行本

著者名	論文タイトル名	書籍名	編集者名	出版社名	出版地	出版年	ページ
Machida A, Ohkubo T, Yokota T.	Circulating MicroRNAs in the Cerebrospinal Fluid of Patients with Brain Diseases	Circulating MicroRNAs: Methods and Protocols (Methods Mol Biol.)	Kosaka N.	Humana Press		2013	203-9
新井哲明	抗認知症薬および脳循環・代謝改善薬	精神・神経の治療薬事典	樋口輝彦	総合医学社	東京	2013	300-5
新井哲明	ピック病型認知症	ICD-10 精神科診断ガイドブック	岡崎祐士	中山書店	東京	2013	49-63
Bolsover et al.	19章 真核細胞における細胞周期と細胞数制御	基礎コース細胞生物学	永田恭介	東京化学同人	東京	2013	228-242

3R and 4R tau isoforms in paired helical filaments in Alzheimer's disease

Masato Hasegawa · Sayuri Watanabe · Hiromi Kondo · Haruhiko Akiyama · David M. A. Mann · Yuko Saito · Shigeo Murayama

Received: 20 August 2013 / Revised: 29 September 2013 / Accepted: 30 September 2013 / Published online: 9 November 2013
© The Author(s) 2013. This article is published with open access at Springerlink.com

Isoform-specific tau antibodies RD3 and RD4 are useful tools for investigating expression and localization of three-repeat (3R) and four-repeat (4R) tau isoforms. Recently, transition from 3R to 4R tau in Alzheimer's disease (AD) was proposed based on immunohistochemical studies with RD3 and RD4 [3]. Here, we show that two factors influence immunoreactivity to these antibodies. First, deamidation at the RD4 epitope abrogates immunoreactivity to RD4, and second, presentation of RD3 and RD4 epitopes is reciprocally affected by protease. Asparagine at position 279 in the RD4 epitope is predominantly deamidated to aspartic acid in pathological tau in AD brains [2, 4]. Consequently, the

presence of 4R tau in AD pathologies may be underestimated when RD4 is used. However, anti-4R (available from Cosmo Bio Co., Ltd.) raised against RD4 peptide with N279D substitution stained both wild-type and deamidated 4R tau, and strongly stained RD3+/RD4- tangles and smearing tau fragments in Sarkosyl-insoluble fraction of AD brain [2].

It was reported that RD3 stained abundant ghost tangles in entorhinal cortex and tangles in CA1, but failed to stain fine processes of tangles and threads [3], while RD4 failed to detect ghost tangles in entorhinal cortex [3]. To understand these findings, we examined the influence of protease on immunoreactivity. Paraffin sections of AD brains were treated with 10 µg/mL Proteinase K (Pro-K) for 30 min after autoclaving (Ac) and formic acid (FA) treatment. RD3 staining was strongly enhanced (Fig. 1a, b). Conversely, RD4 immunoreactivity almost completely disappeared after Pro-K treatment (Fig. 1c, d). Not only ghost tangles but also RD3-/RD4+ tangles and their processes became RD3-positive after Pro-K treatment (Fig. 1a, b), strongly suggesting that the RD3 epitope was buried in tau filaments of intracellular tangles and threads, and was exposed by Pro-K treatment. Contrary to expectation, anti-4R staining was also enhanced by Pro-K treatment (Fig. 1e, f). It is possible that the recognition site of anti-4R is distinct from that of RD4 and is exposed by Pro-K treatment of sections. Anti-4R antibody may recognize the carboxyl-half of the antigen peptide, while RD4 recognizes the amino-terminal half around N279. Pro-K treatment was also effective in immunostaining of free-floating AD sections with a lower concentration.

To confirm these findings biochemically, Sarkosyl-insoluble fractions from two AD brains were treated with trypsin or Pro-K, then immunoblotted with RD3, RD4, anti-4R and anti-pS396 (Fig. 1g–j). RD3 strongly stained many bands and smears, as seen with pS396 (Fig. 1g, j),

M. Hasegawa (✉) · S. Watanabe
Department of Neuropathology and Cell Biology, Tokyo Metropolitan Institute of Medical Science, Setagaya-ku, Tokyo 156-8506, Japan
e-mail: hasegawa-ms@igakuken.or.jp

H. Kondo
Histology Center, Tokyo Metropolitan Institute of Medical Science, Setagaya-ku, Tokyo 156-8506, Japan

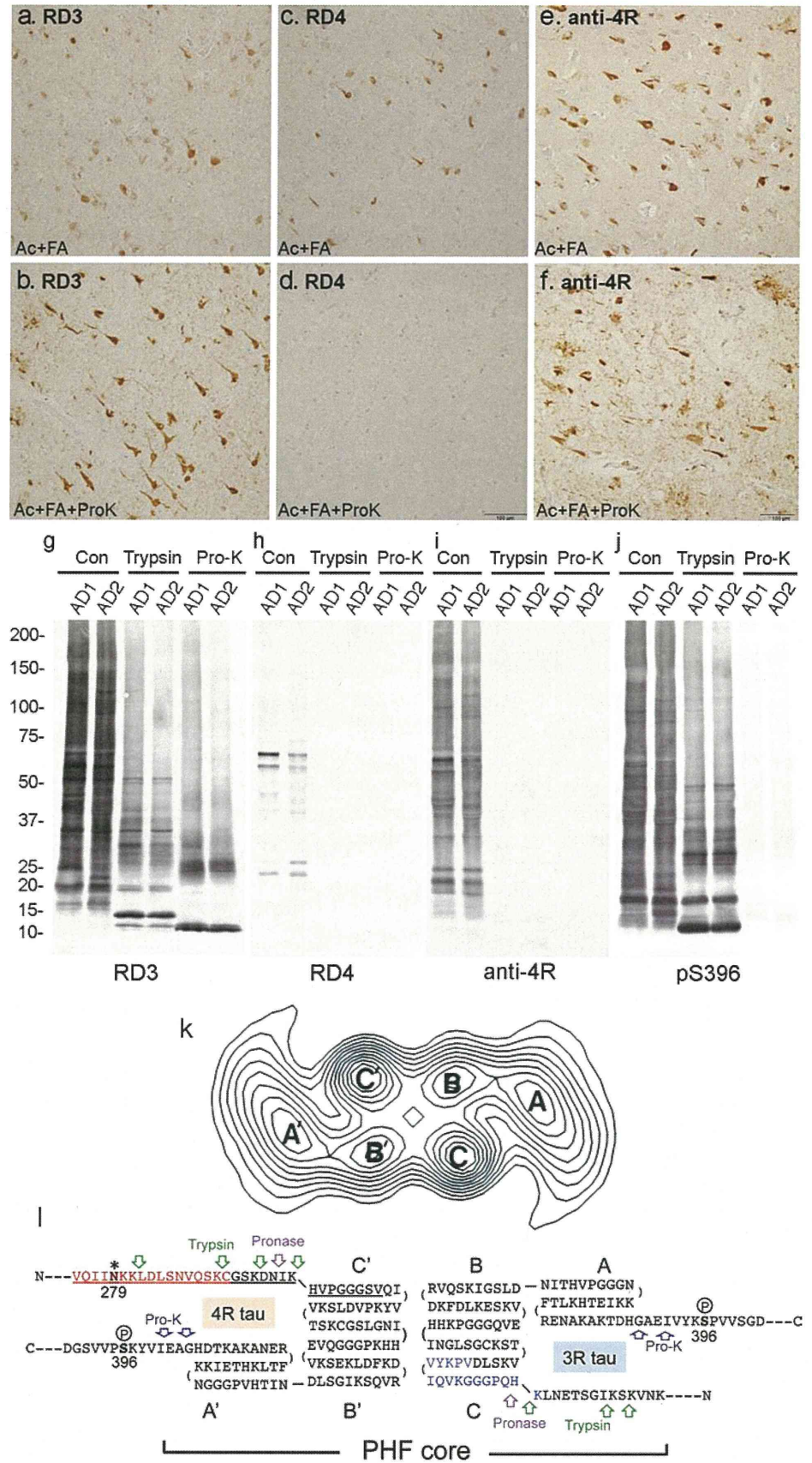
H. Akiyama
Dementia Research Project, Tokyo Metropolitan Institute of Medical Science, Setagaya-ku, Tokyo 156-8506, Japan

D. M. A. Mann
Centre for Clinical and Cognitive Neuroscience, Institute of Brain Behavior and Mental Health, University of Manchester, Salford M6 8HD, UK

Y. Saito
Department of Laboratory Medicine, National Center Hospital, NCNP, 4-1-1 Ogawahigashi, Kodaira, Tokyo 187-8502, Japan

S. Murayama
Department of Neuropathology, Tokyo Metropolitan Institute of Gerontology, Itabashi-ku, Tokyo 173-0015, Japan

Fig. 1 a–f Immunostaining of AD sections after Ac and FA treatment before (**a, c, e**) and after (**b, d, f**) Pro-K treatment, using RD3 (**a, b**), RD4 (**c, d**) and anti-4R (**e, f**). *Bar* 100 μ m. **g–j** Immunoblots of Sarkosyl-insoluble tau from two AD brains, before (*Con*) and after treatments with trypsin or Pro-K, using RD3 (**g**), RD4 (**h**), anti-4R (**i**) and pS396 (**j**). **k–l** Computed cross-section through a paired helical filament (**k**) [reproduced from Ref. [1], with permission of the publisher], a predicted folding model of 3R and 4R tau in PHF (**l**). RD3 and RD4 epitopes are indicated by *blue* and *red*, respectively. 4R tau specific insertion is indicated by *underlining*. The deamidation site N279 is indicated by *asterisks*. Phosphorylation of Ser396 is indicated by *asterisks*. Phosphorylation of Ser396 is indicated. Possible trypsin, pronase and Pro-K cleavage sites are indicated in *green*, *purple* and *dark blue arrows*, respectively. The protease-resistant domain of PHF is indicated as *PHF-core*



whereas RD4 only labeled the 64/68 kDa doublet and some fragments at ~25 kDa (Fig. 1h). Anti-4R strongly stained the smears and fragments (Fig. 1i), suggesting that tau in these RD4-negative anti-4R-positive bands and smears is deamidated at N279. The weak RD4 and strong anti-4R immunoreactivities were completely abolished after trypsin or Pro-K treatment (Fig. 1h, i). This result is inconsistent with the immunohistochemistry, but protease sensitivity is likely different in fixed tissues. In contrast, the RD3 epitope was retained in the fragments, and RD3 strongly reacted with the protease-resistant 10–25 kDa bands after trypsin or Pro-K treatment (Fig. 1g). pS396 epitope was removed by Pro-K but not trypsin, suggesting a location outside the PHF core. Trypsin may not cleave the KSP site because of phosphorylation of Ser396. These results demonstrate reciprocal effects of protease treatment on RD3 and RD4 epitopes, indicating that RD4 epitope in tau in AD is susceptible to proteases, while RD3 epitope is highly resistant.

These results are consistent with previous findings. Wischik et al. identified two types of amino acid sequences, QPGGGKVQIVYK... (3R tau) and IKXVPGG... (4R tau), in 12-kDa tau fragment comprising the pronase-resistant core of PHFs [6] (see Fig. 1k). We identified HQPGGG... (3R tau) and HVPGGG... (4R tau) in 7–15 kDa trypsin-resistant fragments of PHF-tau in AD brains [5]. In both cases, 3R and 4R tau isoforms were detected, but the 4R tau N-terminus lacked the RD4 epitope. Based on these observations and a computed cross-section of PHF (Fig. 1k) [1], we propose a schematic model of tau folding in PHF (Fig. 1l). Analysis of the cross-sectional density in the PHF core on electron micrographs indicates the presence of two C-shaped morphological units, which correspond to the two strands of PHF, each with three domains (Fig. 1k) [1]. The RD3 epitope is buried in the PHF core and is normally masked by the N- or C-terminal region of tau, but is exposed in ghost tangles and/or in PHFs attacked by proteases. The RD4 epitope, which is mostly deamidated in PHF, is located slightly outside the core, where it can be digested by proteases (Fig. 1l). This model can explain the epitope masking of RD3 and RD4 and the reciprocal effects of degradation or protease treatment on the immunoreactivities.

This study indicates that differential presentation of epitopes can occur as a result of folding and processing,

even when the epitopes are located in close proximity. Tau in PHFs appears to be processed gradually by intracellular proteases and more extensively in extracellular space during AD progression. We suggest that changes in immunoreactivity to antibodies reflect aging of tau in tangles or PHFs, which are composed of both 3R and 4R tau isoforms. We also show that Pro-K treatment of sections after Ac and FA treatment is useful for unmasking buried epitopes.

Acknowledgments We acknowledge the support of Alzheimer's Research UK and Alzheimer's Society through their funding of Manchester Brain Bank under the Brains for Dementia Research (BDR) initiative. This work was supported by Grants-in-Aid for Scientific Research (S) (JSPS KAKENHI 23228004), (A) (JSPS KAKENHI 23240050), and MHLW Grant 12946221 (to M.H.).

Open Access This article is distributed under the terms of the Creative Commons Attribution License which permits any use, distribution, and reproduction in any medium, provided the original author(s) and the source are credited.

References

1. Crowther RA (1991) Straight and paired helical filaments in Alzheimer disease have a common structural unit. *Proc Natl Acad Sci USA* 88:2288–2292
2. Dan A, Takahashi M, Masuda-Suzukake M, Kametani F, Nonaka T, Kondo H, Akiyama H, Arai T, Mann DM, Saito Y, Hatsuta H, Murayama S, Hasegawa M (2013) Extensive deamidation at asparagine residue 279 accounts for weak immunoreactivity of tau with RD4 antibody in Alzheimer's disease brain. *Acta Neuropathol Commun* 1:54
3. Hara M, Hirokawa K, Kamei S, Uchihara T (2013) Isoform transition from four-repeat to three-repeat tau underlies dendrosomatic and regional progression of neurofibrillary pathology. *Acta Neuropathol* 125:565–579
4. Hasegawa M, Morishima-Kawashima M, Takio K, Suzuki M, Titani K, Ihara Y (1992) Protein sequence and mass spectrometric analyses of tau in the Alzheimer's disease brain. *J Biol Chem* 267:17047–17054
5. Hasegawa M, Watanabe A, Takio K, Suzuki M, Arai T, Titani K, Ihara Y (1993) Characterization of two distinct monoclonal antibodies to paired helical filaments: further evidence for fetal-type phosphorylation of the tau in paired helical filaments. *J Neurochem* 60:2068–2077
6. Wischik CM, Novak M, Thogersen HC, Edwards PC, Runswick MJ, Jakes R, Walker JE, Milstein C, Roth M, Klug A (1988) Isolation of a fragment of tau derived from the core of the paired helical filament of Alzheimer disease. *Proc Natl Acad Sci USA* 85:4506–4510

RESEARCH

Open Access

Dipeptide repeat proteins are present in the p62 positive inclusions in patients with frontotemporal lobar degeneration and motor neurone disease associated with expansions in *C9ORF72*

David MA Mann^{1*}, Sara Rollinson², Andrew Robinson¹, Janis Bennion Callister², Jennifer C Thompson¹, Julie S Snowden¹, Tania Gendron³, Leonard Petrucelli³, Masami Masuda-Suzukake⁴, Masato Hasegawa⁴, Yvonne Davidson¹ and Stuart Pickering-Brown²

Abstract

Background: Cases of Frontotemporal Lobar Degeneration (FTLD) and Motor Neurone Disease (MND) associated with expansions in *C9ORF72* gene are characterised pathologically by the presence of TDP-43 negative, but p62 positive, inclusions in granule cells of the cerebellum and in cells of dentate gyrus and area CA4 of the hippocampus.

Results: We screened 84 cases of pathologically confirmed FTLD and 23 cases of MND for the presence of p62 positive inclusions in these three brain regions, and identified 13 positive cases of FTLD and 3 of MND. All cases demonstrated expansions in *C9ORF72* by Southern blotting where frozen tissues were available. The p62 positive inclusions in both cerebellum and hippocampus were immunostained by antibodies to dipeptide repeat proteins (DPR), poly Gly-Ala (poly-GA), poly Gly-Pro (poly-GP) and poly Gly-Arg (poly-GR), these arising from a putative non-ATG initiated (RAN) sense translation of the GGGGCC expansion. There was also some slight, but variable, immunostaining with poly-AP antibody implying some antisense translation might also occur, though the relative paucity of immunostaining could reflect poor antigen avidity on the part of the antisense antibodies. Of the FTLD cases with DPR, 6 showed TDP-43 type A and 6 had TDP-43 type B histology; one had FTLD-tau with the pathology of corticobasal degeneration. There were no qualitative or quantitative differences in the pattern of immunostaining with antibodies to DPR, or p62, proteins between TDP-43 type A and type B cases. Ratings for frequency of inclusions immunostained by these poly-GA, poly-GP and poly-GR antibodies broadly correlated with those for immunolabelled by p62 antibody in all three regions.

Conclusion: We conclude that DPR are a major component of p62 positive inclusions in FTLD and MND.

Keywords: Frontotemporal lobar degeneration, *C9ORF72*, p62 inclusions, Dipeptide repeat proteins

Background

Frontotemporal Lobar Degeneration (FTLD) is a clinical, pathological and genetically heterogeneous condition. The major clinical syndromes principally involve personality and behavioural change (behavioural variant frontotemporal dementia, or bvFTD) or language alterations of a fluent

(semantic dementia) or non-fluent (progressive non-fluent aphasia) nature [1]. All three syndromes can be accompanied by Motor Neurone Disease (MND) though the combination of FTD and MND is most common. Histologically, around half of cases have tau-based pathology, half have TDP-43-based pathology, and about 5% have FUS-based pathology [2,3]. Importantly, around 40% of all cases have a strong family history of similar disease, irrespective of clinical or histological subtype [1].

By 2007, causative mutations had been identified in tau (*MAPT*) [4] and progranulin (*GRN*) [5,6]. Nonetheless, it

* Correspondence: david.mann@manchester.ac.uk

¹Clinical and Cognitive Sciences Research Group, Institute of Brain, Behaviour and Mental Health, Faculty of Medical and Human Sciences, University of Manchester, Salford Royal Hospital, Salford M6 8HD, UK
Full list of author information is available at the end of the article

was well known at that time that a number of large, independent FTD + MND kindreds demonstrated linkage to chromosome 9 in the region 9p21.2-p13.3 [7-10]. Subsequently, three GWAS studies for MND [11-13], and one for FTLD [14] identified a susceptibility locus within this linked region, with strongest association coming from a 80 kb haplotype block containing 3 genes, *MOBK2B*, *IFNK* and *C9ORF72*. It has now been shown that this at least some of this association is due to the presence of a large hexanucleotide (GGGGCC) in *C9ORF72* gene in patients with both FTLD and MND [15,16]. The expansion occurs in the first intron or the promoter region of the gene, depending upon the transcript isoform in question, and can number up to as many as 1500 repeats. The expansion is found in about one in every twelve patients with FTLD, but this varies depending on geographical region with the expansion being rare in Asia [16].

Pathologically, most FTLD cases with the expansion [15-20], like many non-mutational cases of FTLD [2,21,22], show inclusion bodies within neurones (NCI) and glial cells of the cerebral cortex and hippocampus that contain the nuclear transcription factor, TDP-43, and are said bear a TDP-43 histological subtype termed FTLD-TDP type B (according to [23]), compatible with a clinical diagnosis of FTD and MND. Others, however, show a TDP-43 histological type characterised by the presence of many short neurites (DN) along with NCI within the outer layers of the cerebral cortex, and termed FTLD-TDP type A [23]. Nonetheless, irrespective of TDP-43 histological type, expansion carriers also show a unique pathology within the hippocampus [17] and cerebellum [17-19,24] characterised by NCI that are TDP-43 negative, but immunoreactive to p62 protein.

P62 is a marker for proteins destined for proteasomal degradation though the precise target protein within such NCI remains uncertain, and the pathogenetic mechanism underlying the hexanucleotide expansion remains unclear. Nonetheless, this is likely to result from one, or a combination, of three possible mechanisms: i) haploinsufficiency leading to loss of *C9orf72* protein [15,16], ii) the expansion might form nuclear foci of toxic RNA and sequester other RNA-binding proteins such as Pur Alpha (Pur α) [25], or iii) RAN (repeat associated non ATG-initiated) translation of the expanded repeat region may lead to the 'inappropriate' formation of dipeptide repeat proteins (DPR) which may aggregate and confer neurotoxicity [26,27].

Here, we show that DPR are at least one of the target protein(s) within the TDP-43 negative, p62-positive NCI in cases of FTLD associated with hexanucleotide (GGGGCC) expansions, and that such peptides are not associated with other histological forms, or genetic subtypes, of FTLD.

Methods

Patients

Brain tissues were available in the Manchester Brain Bank from a series of 84 patients with FTLD and 23 with MND. All patients were from the North West of England and North Wales. All FTLD cases fulfilled Lund-Manchester clinical diagnostic criteria for FTLD [28,29], and all those with MND fulfilled El Escorial criteria [30]. All brains had been obtained with full ethical permission following consent by the next of kin.

Histological methods

Serial paraffin sections were cut (at a thickness of 6 μ m) from formalin fixed blocks of temporal cortex (with hippocampus) and cerebellar cortex. Sections within the series were immunostained by routine methods for amyloid β protein (A β), tau, TDP-43 and FUS proteins, employing microwaving in 0.1 M citrate buffer, pH 6.0 for antigen retrieval [2]. Pathologically, of the 84 patients with FTLD, 30 had FTLD-tau (9 with FTLD-tau Picks (PiD), 7 with *MAPT* mutation, 11 with CBD and 3 with PSP), 52 had FTLD-TDP (24 with type A histology, 22 with type B histology, 6 with type C histology), 1 had FTLD-FUS (aFTLD-U) and 1 had FTLD-ni. (see [23] for definitions).

Further sections from each case within the series were screened for the presence of p62-immunoreactive NCI by immunostaining with p62-lck ligand (rabbit polyclonal antibody (B D Biosciences, Oxford, UK) 1:100) employing a standard ABC Elite kit (Vector, Burlingame, CA, USA) with DAB as chromagen, and again microwaving in 0.1 M citrate buffer, pH6.0 for antigen retrieval. Positive cases were defined where p62 positive, TDP-43 negative NCI within either the cerebellum (see [18]) or hippocampus (see [17]) could be clearly seen under low power objective (\times 20) and the majority of high power fields (\times 40) contained at least 2 NCI. Negative cases were either completely devoid of p62 immunostaining, or small amounts of apparently extracellular and 'extraneous' p62 positive particulate material was observed in occasional high power fields.

Dipeptide antibody staining

A non-ATG initiated translation of the expansion would putatively result in DPRs derived from either from forward (sense) (poly Gly-Pro, (poly-GP), poly Gly-Ala (poly-GA) and poly Gly-Arg, (poly-GR)) or reverse (antisense) (poly Ala-Pro (poly-AP), poly Pro-Gly (poly-PG) and poly Pro-Arg (poly-PR)) directions. Consequently, we commissioned a series of custom made rabbit polyclonal antibodies, raised against such putatively translated proteins. Briefly, peptides consisting of 15 repeats with an additional N terminal cysteine were synthesised and N-terminally conjugated to keyhole limpet haemocyanin prior to immunisation. All steps in the preparation were performed

by Genentech. Antibodies were successfully raised against poly-GP, poly-GR, poly-AP and poly-PR proteins. However, it was not possible to generate antibodies to poly-GA and poly-PG proteins.

Serial sections from those cases showing p62-positive pathology, and those from 11 (non-p62 positive) cases with other histological and genetic forms of FTLD, other neurodegenerative disorders and healthy controls (see Table 1) were immunostained for DPR. Antibodies were employed in standard IHC (as above) though, in this instance, antigen unmasking was performed by pressure cooking in citrate buffer (pH 6, 10 mM) for 30 minutes, reaching 120 degrees Celsius and >15 kPa pressure. Following titration to determine optimal immunostaining, antibodies were employed at dilutions of 1:500 (poly-AP and poly-PR), 1:750 (poly-GR) or 1:2000 (poly-GP).

Further sections from the series were immunostained with poly-GA (and poly-GP and poly-GR) antibodies courtesy of Dr M Hasegawa. These antibodies were raised against poly-(GA)₈, poly-(GP)₈ and poly-(GR)₈ peptides with cysteine at N-terminus. The peptides were conjugated to *m*-maleimidobenzoyl-*N*-hydrosuccinimide ester-activated thyroglobulin. The thyroglobulin-peptide complex (200 µg) emulsified in Freund's complete adjuvant was injected subcutaneously into a New Zealand White rabbit, followed by 4 weekly injections of peptide complex emulsified in Freund's incomplete adjuvant, starting after 2 weeks after the first immunization. Immunoreactivities of these antisera were characterized by ELISA as follows. The peptide immunogens were coated onto microtiter plates. The plates were blocked with 10% fetal bovine serum (FBS) in PBS, incubated with the rabbit antisera diluted in 10% FBS/PBS at room temperature for 1.5 h, followed by incubation with HRP-goat anti-rabbit IgG (Bio-Rad) at 1:3000 dilution, and reacted with the substrate, 0.4 mg/mL *o*-phenylenediamine, in citrate phosphate buffer (24 mM citric acid, 51 mM Na₂HPO₄). The absorbance at 490 nm was measured using Plate Chameleon (HIDEX). All antibodies were used for immunohistochemistry at dilution of 1:2000, and pretreated as above. Sections were also immunostained with the anti-dipeptide repeat antibody C9RANT [26] (gift from L Petrucelli) at 1:3000 dilution.

Microscopic analysis

Sections of cerebellum and hippocampus immunostained for p62 and each of our own 4 DPR antibodies, and the poly-GA antibody supplied by M Hasegawa were assessed for the presence of DPR immunostained NCI within granule cells of the cerebellum, and dentate gyrus cells and CA4 pyramidal cells of the hippocampus at ×20 magnification. The frequency of DPR-immunoreactive NCI was assessed according to:

0 = no immunostained NCI present in any field.

1 = very few immunostained NCI present, in some but not all fields.

2 = a moderate number of immunostained NCI present in each field.

3 = many immunostained NCI present affecting most cells in each field.

4 = very many immunostained NCI present, affecting nearly all cells in every field.

Southern blotting

Frozen brain tissue for Southern blotting was available for most cases employed in the study. Southern blotting was performed using a PCR DIG labelled probe adjacent to the expansion. The PCR probe consisted of 851 bp amplicon using the following primers, forward 5' CCCACACCTGC TCTTGCTA 3'; reverse 5' CGTTCTGTGTGATTTTGA GTGATGA 3'.

Briefly, samples were digested overnight with 20 u of XbaI (New England Biolabs). Samples were electrophoresed in 0.8% agarose 1 xTBE gels run at 1.5 volts/cm for 18 hours. Following standard protocols [31], gDNA was transferred to positively charged nylon membrane. Membranes were fixed using UV light at 365 nm for 3 minutes using a GE Image quant 350. Membranes were hybridized and detected as per the DIG detection Manual (Roche Applied Science). Signals were visualised using the GE Image quant 350 after 1 to 4 hours.

Expansion sizing and analysis

Expansion sizing was carried out using ImageQuant TL software (Version 7, GE Healthcare) sizing the repeat number against the DIG labelled lambda Hind III labelled size standard included on each gel (Roche Applied Science). Positive control (gDNA isolated from the B-Lymphocyte cell line ND06769 obtained from the NINDS Repository-Coriell) and negative control were included on each blot, and were required to show a band of the expected size or no signal on hybridisation respectively for each blot to pass quality control.

Statistical analysis

Rating data from semiquantitative assessments was entered into an excel spreadsheet and analysed using Statistical Package for Social Sciences (SPSS) software (version 17.0). Mann-Whitney test was used to compare rating data between pairs of groups. A p-value of less than 0.05 was considered statistically significant. Regression analysis using Intercooled Stata Version 9 (StataCorp) was carried out to investigate effects between repeat length, age of onset and disease duration.

Results

Screening the 84 FTLD and 23 MND cases with p62 revealed 16 cases, 13 with FTLD (cases #1-13) and 3

Table 1 Selected clinical and pathological details of cases investigated by dipeptide immunostaining

Case	M/F	Clinical diagnosis	Pathological diagnosis	Family history	Onset (y)	Duration (y)	Brain weight (g)
1	M	FTD	FTLD-TDP type A	2 brothers, 2 sisters FTD	49	9	1050
2	M	FTD	FTLD-TDP type A	brother MND**, mother and grandmother FTD	60	8	1210
3	F	FTD	FTLD-TDP type A	none available	59	5	1140
4	M	FTD	FTLD-TDP type A	father dementia	64	8	1100
5	M	FTD	FTLD-TDP type A	father similar presentation, paternal grandmother 'AD'	63	2	na
6	M	FTD	FTLD-TDP type A	yes	78	4	1200
7	M	FTD + MND	FTLD-TDP type B	?paternal aunt said to be 'strange'	60	2	na
8	M	FTD + MND	FTLD-TDP type B	mother FTD	57	2	1210
9	M	FTD	FTLD-TDP type B	mother dementia	54	12	na
10	F	FTD	FTLD-TDP type B	mother and sister FTD	51	19	na
11	F	FTD + MND	FTLD-TDP type B	father 'AD', sister MND, paternal nephew MND	63	2	na
12	F	FTD + MND	FTLD-TDP type B	sister MND, brother FTD, mother 'multiple sclerosis'	68	5	1363
13	M	FTD	Corticobasal degeneration	father and 5 sisters had Huntington's disease	59	70	1271
14	M	MND	MND	brother FTD**, mother and grandmother FTD	60	5	1350
15	F	MND	MND	none available	40	5	1330
16	M	MND	MND	brother MND, sister FTD + MND	53	2	1250
17	M	FTD	FTLD-tau Pi	none	69	6	na
18	F	FTD	FTLD-tau MAPT +16	mother: early onset dementia; brother: MND	48	15	1100
19	M	Corticobasal Syndrome	FTLD-tau CBD	none	65	na	1020
20	M	FTD	FTLD-TDP A	mother AD, brother AD (but with behavioural problems)	66	7	980
21	F	FTD + MND	FTLD-TDP B	none available	50	2	1050
22	F	SD	FTLD-TDP C	none	70	2	1522
23	F	Alzheimer's disease	Alzheimer's disease	none	74	12	1220
24	M	Huntington's disease	Huntington's disease	none available	48	24	na
25	M	Huntington's disease	Huntington's disease	none available	56	19	1340
26	M	Normal	Normal control	none	54*	na	1720
27	F	Normal	Normal control	none	53*	na	1220

FTD = Frontotemporal dementia; MND = Motor Neurone Disease; SD = semantic dementia; FTLD = Frontotemporal Lobar Degeneration; na = data not available/applicable; * = age at death; ** = cases #2 and 14 were brothers.

with MND (cases #14-16) (Table 1) showing p62 positive, TDP-43 negative NCI within granule cells of the cerebellum and other cerebellar cell types, and in granule cells of the dentate gyrus, and pyramidal cells of CA4, CA3 and CA2 regions of the hippocampus, as described previously [17-19,24]. Twelve of the 13 FTLD cases showed TDP-43 proteinopathy, classifiable [23] as either type A (6 cases) or type B (6 cases): the other case had tauopathy compatible with corticobasal degeneration (CBD) (Table 1). Eight of the FTLD cases had presented with bvFTD clinically, 4 with FTD + MND and one (with CBD pathology) with a combination of FTD and corticobasal syndrome. All MND cases bore typical TDP-43 pathological changes in motor neurones of brain stem nuclei and spinal cord (where this was available for analysis).

Frozen tissue was available for 12 of the 16 cases showing p62 pathological changes in cerebellum and hippocampus. These included 9 cases with FTLD (cases #1-3, 7, 9-13) and all 3 cases with MND (cases #14-16) (Table 1). All 12 of these cases demonstrated a pathological expansion in *C9ORF72* by Southern blotting. Expansion size ranged from ~5 kb (~450 repeats) to in excess of 23 kb (over 3600 repeats) (Figure 1). No expansions were detected in cases where no p62 pathological changes were observed. There was no correlation between repeat size and age of disease onset or duration (see Additional file 1: Figure S1).

p62 immunostaining

In FTLD cases, on p62 immunostaining, NCI in granule cells of the cerebellum appeared as small rounded or oat-shaped bodies, though occasionally larger, more rounded and solid NCI were observed (Figure 2a). These were very abundant in case #1, common in cases #4, 7 and 10, moderately plentiful in cases #2 and 5, occasional in cases #3, 8 and 12, and rare in cases #6, 9 and 11 (Table 2). Similar, more granular, NCI were usually present in basket cells (Figure 2b), especially when granule cell

inclusions were frequent, but none were seen within Golgi neurones, or within Bergmann glia. In some cases, occasional Purkinje cells (Figure 2c) and neurones in the dentate nucleus (Figure 2d) contained small, spicular or granular p62-immunoreactive structures, but these were not immunoreactive with TDP-43 antibodies. In most cases, occasional cells resembling astrocytes were seen to contain p62 immunoreactive intranuclear inclusions, these being located deep in the granule cell layer. All cases also showed abundant, small, rounded NCI within granule cells of the dentate gyrus (Figure 2e), along with spicular or granular inclusions within pyramidal cells of areas CA2/3 and CA4 (Figure 2f), less commonly in CA1 and subiculum (Table 2).

In MND cases, cerebellar granule cell NCI were abundant in cases #14 and 16, but were rare in case #15 (Table 2). In all cases, p62 positive NCI were also observed within granule cells of the dentate gyrus, and similar (to FTLD cases) small, spicular or granular p62-immunoreactive inclusions were seen within pyramidal cells of areas CA2/3 and CA4, less commonly in CA1 and subiculum. Both of these kinds of changes were occasionally present in cases #14 and 15 but were moderately common in case #16 (Table 2).

In all FTLD and MND cases variable, but often many, pyramidal neurones, chiefly within the deeper layers of the adjoining cerebral (temporal) cortex also contained NCI similar to those in the hippocampus CA regions (not shown).

DPR immunostaining

Results of immunostaining for DPR are shown in Table 2. All FTLD and MND cases showed similar patterns of immunostaining though there were quantitative differences between cases with respect to the number of inclusions immunostaining.

As with p62 immunostaining, immunostaining with both our own custom anti poly-GP and poly GR antibodies and

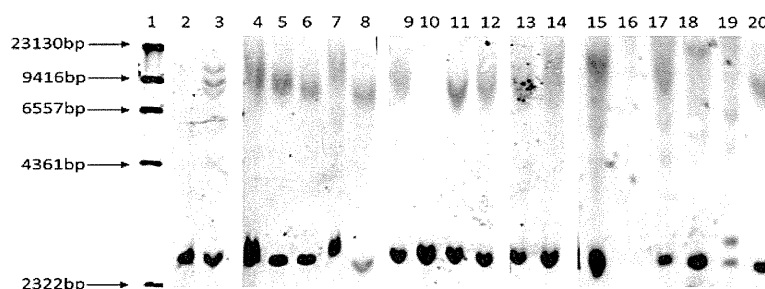


Figure 1 Southern blotting of FTLD and MND cases bearing expansions in *C9ORF72*. Lane 1: Marker, Lane 2: Negative control brain, Lane 3: ND06769, Lane 4: 01/06 FTD case #3, Lane 5: MND case #15, Lane 6: FTD/MND case #11, Lane 7: FTD case #10, Lane 8: CBD case #13, Lane 9: FTD case #1; Lane 10: control FTD case with tauopathy, Lane 11: FTD case #9, Lane 12: FTD/MND case #12, Lane 13: FTD case #2; Lane 14: MND case #14, Lane 15: FTD/MND case #7, Lane 20: MND case#16. Lanes 16-19 show expansions in other clinically diagnosed cases of MND (positive controls) where no brain tissue was available.